

Accepted Manuscript

Identification of new aryl hydrocarbon receptor (AhR) antagonists using live zebrafish model

Jieun Jeong, Kun-Hee Kim, Dong-Young Kim, Gopalakrishnan Chandrasekaran, Minhee Kim, Suvarna H. Pagire, Mahesh Dighe, Eun Young Choi, Su-Min Bak, Eun-Young Kim, Myung-Geun Shin, Seok-Yong Choi, Jin Hee Ahn

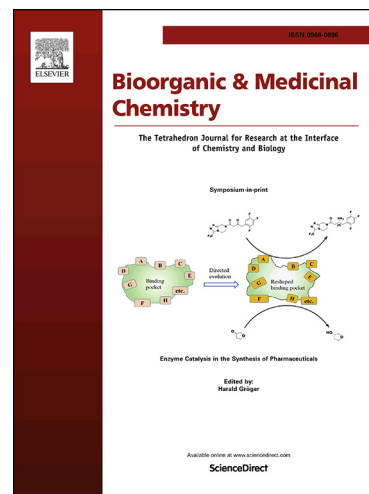
PII: S0968-0896(19)30794-1
DOI: <https://doi.org/10.1016/j.bmc.2019.07.030>
Reference: BMC 15014

To appear in: *Bioorganic & Medicinal Chemistry*

Received Date: 15 May 2019
Revised Date: 11 July 2019
Accepted Date: 17 July 2019

Please cite this article as: Jeong, J., Kim, K-H., Kim, D-Y., Chandrasekaran, G., Kim, M., Pagire, S.H., Dighe, M., Young Choi, E., Bak, S-M., Kim, E-Y., Shin, M-G., Choi, S-Y., Hee Ahn, J., Identification of new aryl hydrocarbon receptor (AhR) antagonists using live zebrafish model, *Bioorganic & Medicinal Chemistry* (2019), doi: <https://doi.org/10.1016/j.bmc.2019.07.030>

This is a PDF file of an unedited manuscript that has been accepted for publication. As a service to our customers we are providing this early version of the manuscript. The manuscript will undergo copyediting, typesetting, and review of the resulting proof before it is published in its final form. Please note that during the production process errors may be discovered which could affect the content, and all legal disclaimers that apply to the journal pertain.



Identification of new aryl hydrocarbon receptor (AhR) antagonists using live zebrafish model

Jieun Jeong,^{1,6} Kun-Hee Kim,^{2,6} Dong-Young Kim,^{3,6} Gopalakrishnan Chandrasekaran,² Minhee Kim,¹ Suvarna H Pagire,¹ Mahesh Dighe,¹ Eun Young Choi,³ Su-Min Bak⁴, Eun-Young Kim⁴, Myung-Geun Shin,^{5,*} Seok-Yong Choi,^{2,*} and Jin Hee Ahn^{1,*}

¹ Department of Chemistry, Gwangju Institute of Science and Technology, Gwangju 61005, Republic of Korea

² Department of Biomedical Sciences, Chonnam National University Medical School, Gwangju, Republic of Korea,

³ Department of Biomedical Sciences, University of Ulsan College of Medicine, Seoul, Republic of Korea

⁴ Department of Life and Nanopharmaceutical Science and Department of Biology, Kyung Hee University, Seoul, Republic of Korea

⁵ Department of Laboratory Medicine, Chonnam National University Medical School, Gwangju, Republic of Korea

*Corresponding authors: e-mail address: jhahn@gist.ac.kr; address: Department of Chemistry, Gwangju Institute of Science and Technology, Gwangju 61005, Republic of Korea, e-mail address: zebrafish@chonnam.ac.kr; address: Department of Biomedical Sciences, Chonnam National University Medical School, Gwangju, Republic of Korea, & e-mail address: mgshin@chonnam.ac.kr; address: Department of Laboratory Medicine, Chonnam National University Medical School, Gwangju, Republic of Korea.

⁶ Authors contributed equally

Abstract

A new series of 1,3-diketone, heterocyclic and α,β -unsaturated derivatives were synthesized and evaluated for their AhR antagonist activity using zebrafish and mammalian cells. Compounds **1b**, **2c**, **3b** and **5b** showed significant AhR antagonist activity in a transgenic zebrafish model. Among them, compound **3b**, and **5b** found to have excellent AhR antagonist activity with IC₅₀ of 3.36 nM and 8.3 nM in luciferase reporter assay. In stem cell proliferation assay, compound **5b** elicited marked HSC expansion.

Keywords: Aryl hydrocarbon receptor (AhR), antagonist, zebrafish, stem cell

1. INTRODUCTION

The aryl hydrocarbon receptor (AhR) is a transcription factor that belongs to a family of basic helix-loop-helix/Per-Arnt-Sim (b-HLH/PAS) proteins^{1,2}. AhR consists of b-HLH and PAS domains. The b-HLH domain is located in the N-terminal region and involved in DNA binding³. The PAS domain has two subdomains. The PAS-A subdomain is responsible for protein dimerization and the PAS-B is implicated in ligand binding⁴. In the absence of its ligand, AhR forms an inactive complex with a heat shock protein 90 (HSP90) dimer and a co-chaperone protein X-associated protein 2 (XAP2) and thus remains in the cellular cytoplasm. The HSP90 dimer protects inactive AhR complex from proteolysis and AhR Nuclear Translocator (ARNT) binding. Ligand binding changes inactive AhR to its active form, resulting in exposure of a nuclear localization signal (NLS) in the PAS domain. Subsequently, the active AhR complex translocates to the nucleus where ARNT displaces HSP90 and XAP2 from the AhR complex by forming an AhR-ARNT heterodimer^{2,5,6}. Further, this heterodimer binds to a dioxin-responsive element (DRE) in the promoters of various genes, thus inducing transcription of these genes that regulate immune, hepatic, cardiovascular and reproductive systems as well as lipid and xenobiotic metabolisms⁷.

The activation of AhR by the ligand including 2,3,7,8-tetrachlorodibenzo-*p*-dioxin (TCDD) and benzo[*a*]pyrene causes dysfunction of cholesterol pathway that leads to formation of atheroma due to accumulation of fats in the blood vessels, thereby resulting atherosclerosis^{8,9}. Also, AhR regulates stem cell proliferation¹⁰. In 2010, Cooke *et al* reported that StemRegenin 1 (SR1), an AhR antagonist, expanded human hematopoietic stem cells (HSCs) *ex vivo*¹¹. Therefore, the development of AhR antagonists would be of great help with the treatment of atherosclerosis and HSC expansion.

Several AhR antagonists including flavones, resveratrol, kaempferol, and pyrazole-5-carboxamide derivatives (Fig. 1) exhibited anti-atherosclerosis effect. However, most of them have not developed further, which prompted us to identify a new series of AhR antagonists.

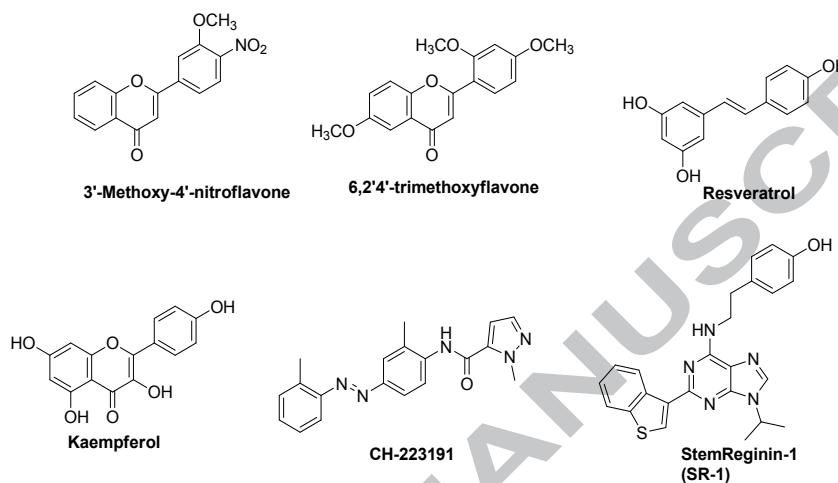


Fig. 1. Reported AhR antagonists.

To identify novel AhR antagonists, we screened a chemical library (6,400 compounds) of Korea Chemical Bank (KCB) using *cyp1a* reporter zebrafish (*Tg(cyp1a:egfp)*)¹². We found compound **1a** having 1, 3-diketone scaffold as a hit compound (Fig. 2). It exhibited moderate AhR inhibitory activity in a zebrafish *in vivo* model. Initial outcome encouraged us to perform scaffold modification for further pharmacophoric exploration.

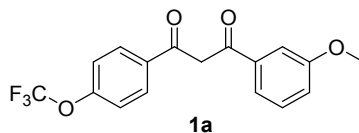
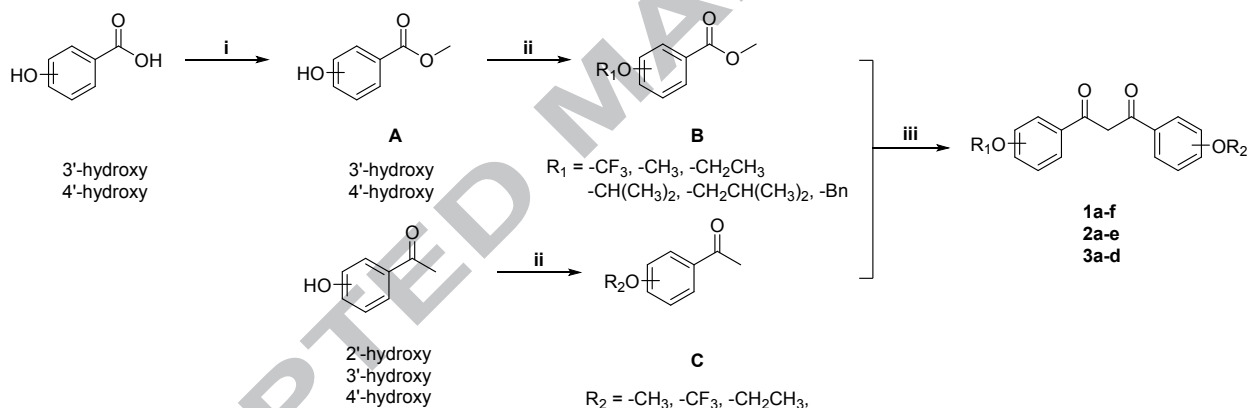


Fig. 2. Structure of hit compound **1a** (GM-90203).

2. Chemistry

Diketone derivatives were synthesized according to Scheme 1. Initially, various methyl alkoxy-benzoate were prepared from different hydroxy benzoic acids through esterification followed by Mitsunobu reaction with various alcohols. Similarly, on other side, different alkoxy-acetophenones were synthesized by carrying out Mitsunobu coupling between various hydroxy acetophenones and alcohols. Subsequently, 1,3-Diketone derivatives (1-3) were synthesized by cross Claisen condensation between various substituted methyl benzoates (B) and acetophenones (C) under basic condition.

Scheme 1. Synthetic route for series 1-3 compounds.

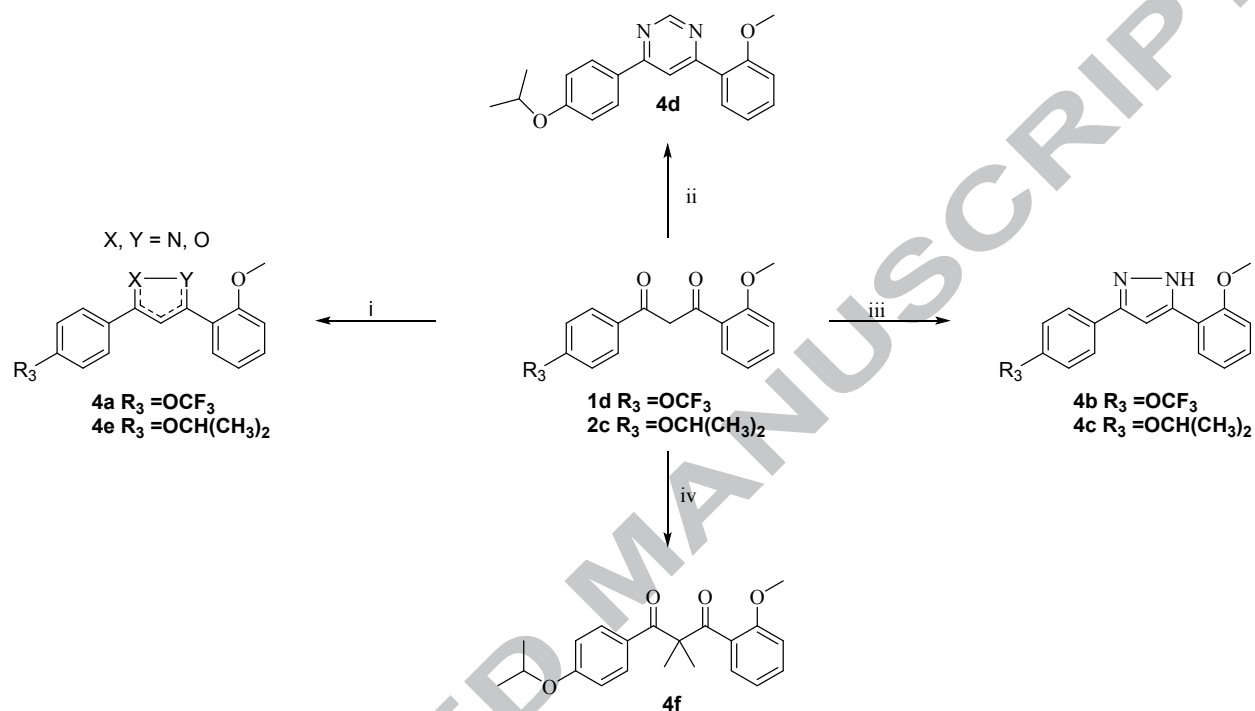


Reagents and condition: i) H_2SO_4 , MeOH, reflux. ii) $\text{R}_1\text{-OH}$ or $\text{R}_2\text{-OH}$, PPh_3 , DIAD, THF, 0°C , RT. iii) NaH, THF, reflux.

Subsequently, heterocyclic compounds and alkylated diketones were synthesized as shown in Scheme 2. 1,3-Diketone derivatives (**1b** and **2c**) reacted with hydroxylamine hydrochloride under reflux to afford respective isoxazole derivatives (**4a** and **4e**). Similarly, **1b** and **2c** reacted with hydrazine hydrate to give pyrazole derivatives (**4b** and **4c**), respectively. Compound **2c**

underwent cyclocondensation with formamidine to give pyrimidine derivative **4d**. Moreover, Compound **2c** underwent methylation to afford dimethyl compound **4f**.

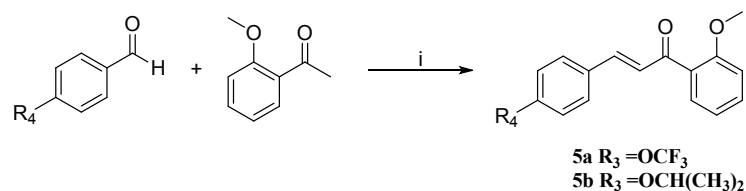
Scheme 2. Synthetic route for series 4 compounds.



Reagents and conditions: i) $\text{NH}_2\text{OH}\cdot\text{HCl}$, EtOH, reflux. ii) formamide, $180\text{ }^\circ\text{C}$, overnight. iii) NH_2NH_2 , EtOH, reflux. iv) CH_3I , NaH, acetone, reflux.

Compounds **5a** and **5b** were synthesized according to scheme 3. They were synthesized by Aldol condensation between respective benzaldehydes and 2-methoxy acetophenones in the presence of sodium hydroxide as a catalyst.

Scheme 3. Synthetic route for series 5 compounds.



Reagents and conditions: i) NaOH, EtOH, 0 °C, room temperature.

3. RESULTS AND DISCUSSION

In the last few decades, zebrafish has emerged as a screening model in drug discovery owing to its significant genomic similarity to human and its transparency during organogenesis that allows for *in vivo* labeling and imaging. Recently, we developed transgenic zebrafish *Tg(cyp1a:egfp)* by incorporating into the zebrafish genome a *cyp1a* fosmid where enhanced green fluorescence protein (EGFP) gene replaced the start codon of *cyp1a*. As *cyp1a* is a target gene of AhR, EGFP fluorescence in *Tg(cyp1a:egfp)* zebrafish can become readout for AhR transcriptional activity. TCDD, an AhR ligand with the highest efficacy, induced EGFP expression in blood vessels, cloaca, gut, lateral line, liver, pectoral fin bud, pronephros, pancreas and swimming bladder of *Tg(cyp1a:egfp)* zebrafish in a dose-dependent manner¹³.

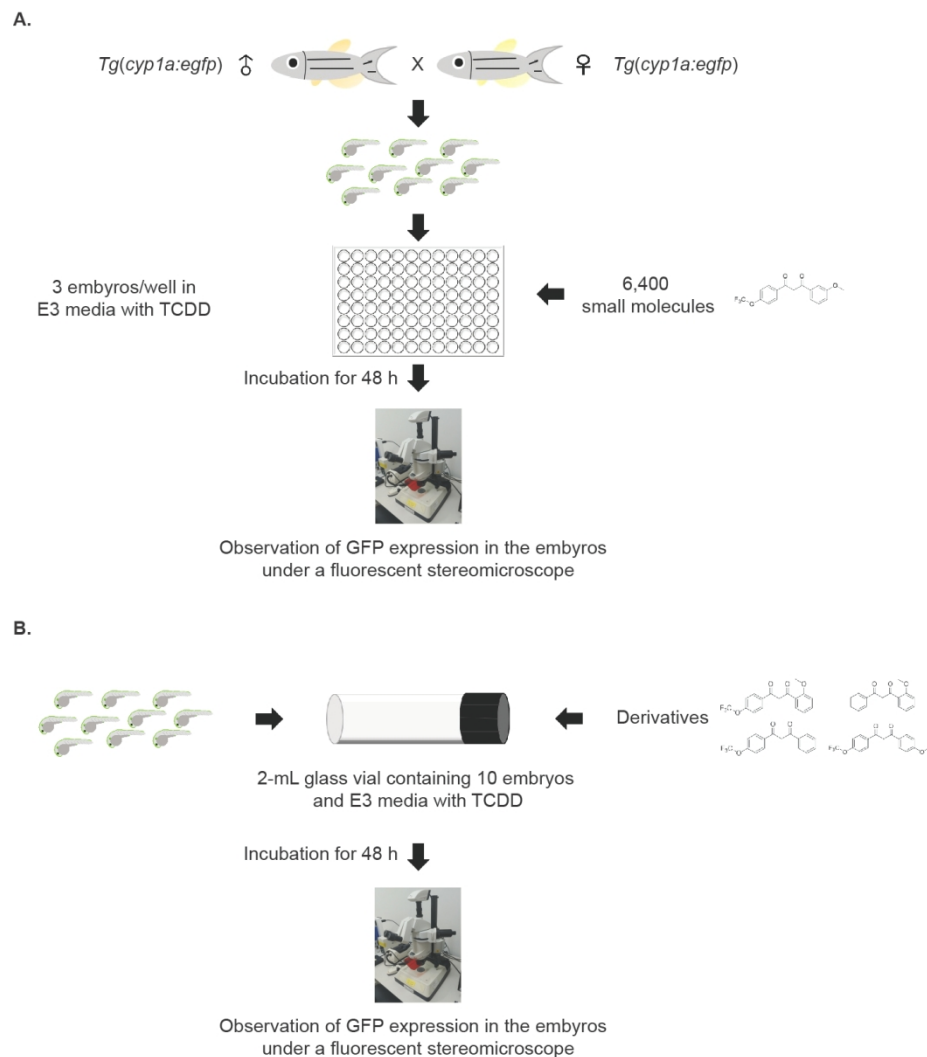
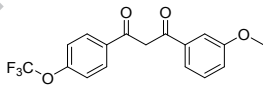
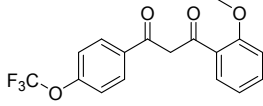
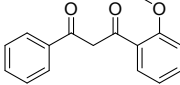


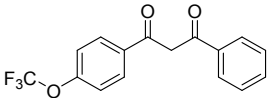
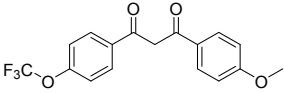
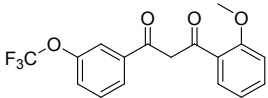
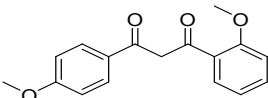
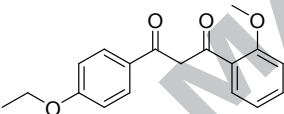
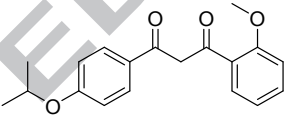
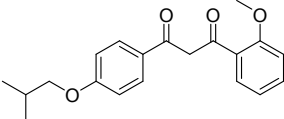
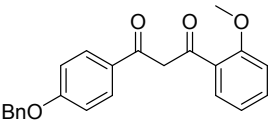
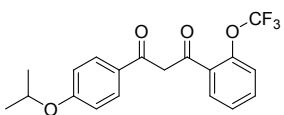
Fig. 3. Fluorescence based screening (A) and optimization (B) for AhR antagonists using *Tg(cyp1a:egfp)* zebrafish.

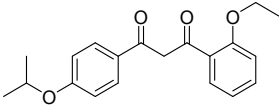
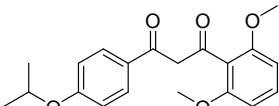
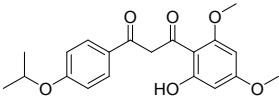
Compound **1a** was identified as a hit through a chemical library screening using the *Tg(cyp1a:egfp)* zebrafish (Fig. 3). **CH223191**, a known AhR antagonist¹², was used as the reference. Optimization of the compound **1a** was performed and the results of the zebrafish study are summarized in Table 1. Compound **1b**, which has *p*-OCF₃ (on left phenyl group) and *o*-OCH₃ (on right phenyl group) substitutions on the phenyl group, showed better antagonistic activity than that of the hit **1a**. However, mono-substituted **1c** and **1d** were not active. Compound **1e**

having *p*-OCF₃ (on left phenyl group) and *p*-OCH₃ (on right phenyl group) substitution showed decreased AhR antagonistic activity. These seemed to suggest that both substituents are necessary for activity. From the above results, we fixed *o*-methoxy group at right phenyl and further modified left phenyl group with diverse substituents. *p*-Methoxy (**2a**), *p*-ethoxy (**2b**), *p*-isopropoxy (**2c**), *p*-isobutyloxy (**2d**) and *p*-benzyloxy (**2e**) derivatives were synthesized and evaluated. Compound **2c** exhibited improved AhR antagonistic activity, whereas methoxy (**2a**), isobutyloxy (**2d**) or benzyloxy (**2e**) derivatives were not active. From the results, we fixed *p*-isopropoxy group at left phenyl and further modified right phenyl group with diverse substituents. Compound **3b** exhibited good AhR antagonist activity. However, di and tri-substituted derivatives (**3c** and **3d**) were not effective.

Table 1. AhR antagonist activity of 1,3-diketone derivatives in a zebrafish model.

Compound	Structure	AhR Antagonist activity* based on fluorescence in <i>Tg(cyp1a:egfp)</i> zebrafish
1a		++
1b		++++
1c		-

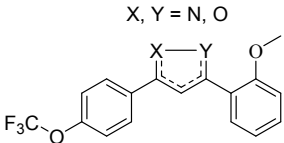
1d		-
1e		-
1f		+
2a		-
2b		+++
2c		++++
2d		-
2e		-
3a		-

3b		++++
3c		-
3d		-

*Excellent (++++), Good (+++), Moderate (++) , Low (+), No (-),

In the preceding study, compounds **1b**, **2c** and **3b** were most active. As they have diketone moiety, we sought more druggable derivatives, which are more rigid with heterocycles and less reactive than diketone moiety, by replacing diketo moiety. Modification of flexible 1,3-diketone to ring closure isoxazole, pyrazole and pyrimidine diminished the AhR antagonist activity compared to **2c** as shown in Table 2. Unfortunately, alkylated diketone derivative (**4f**) was not active either.

Table 2. AhR antagonist activity of heterocyclic and alkylated derivatives in a zebrafish model.

Compound	Structure	AhR Antagonist activity* based on fluorescence in <i>Tg(cyp1a:egfp)</i> zebrafish
4a	<p style="text-align: center;">X, Y = N, O</p> 	-

4b		- (Embryotoxicity)
4c		- (Embryotoxicity)
4d		++
4e		+
4f		-

*Moderate (++) , Low (+) , No (-).

To identify another scaffold, α,β -unsaturated derivatives were synthesized and evaluated for their AhR inhibition. As shown in Table 3, **5b** showed potent AhR inhibition.

Table 3. AhR antagonist activity of α,β -unsaturated derivatives in a zebrafish model.

Compound	Structure	AhR Antagonist activity* based on fluorescence in <i>Tg(cyp1a:egfp)</i> zebrafish
5a		- (Embryotoxicity)
5b		++++

*Excellent (++++),No (-).

From the compounds screening in a zebrafish model, we found that compounds **1b**, **2c**, **3b** and **5b** exerted significant AhR antagonistic activity in a dose-dependent manner (Fig. 4). This finding was validated by Western blotting with anti-GFP antibody showing that compounds **1b**, **2c**, **3b** and **5b** inhibit AhR activity in a dose-dependent manner (Fig. 5).

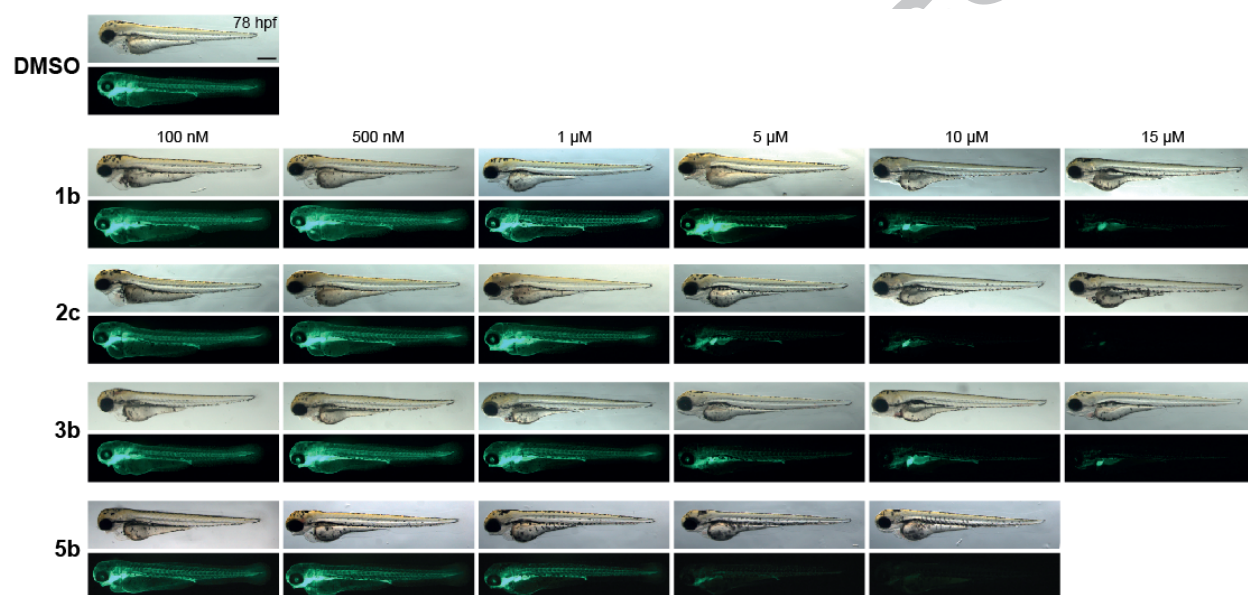


Fig. 4. Assessment of anti-AhR activity of compounds using GFP fluorescence in *Tg(cyp1a:egfp)* zebrafish embryos. *Tg(cyp1a:nls-egfp)* embryos at 30 hours post-fertilization (hpf) were treated for 48 h with TCDD (10 nM) and indicated compound at various concentration and imaged. Upper and lower panels are bright field and fluorescence images, respectively. DMSO was used as vehicle control. Scale bar = 300 μ m.

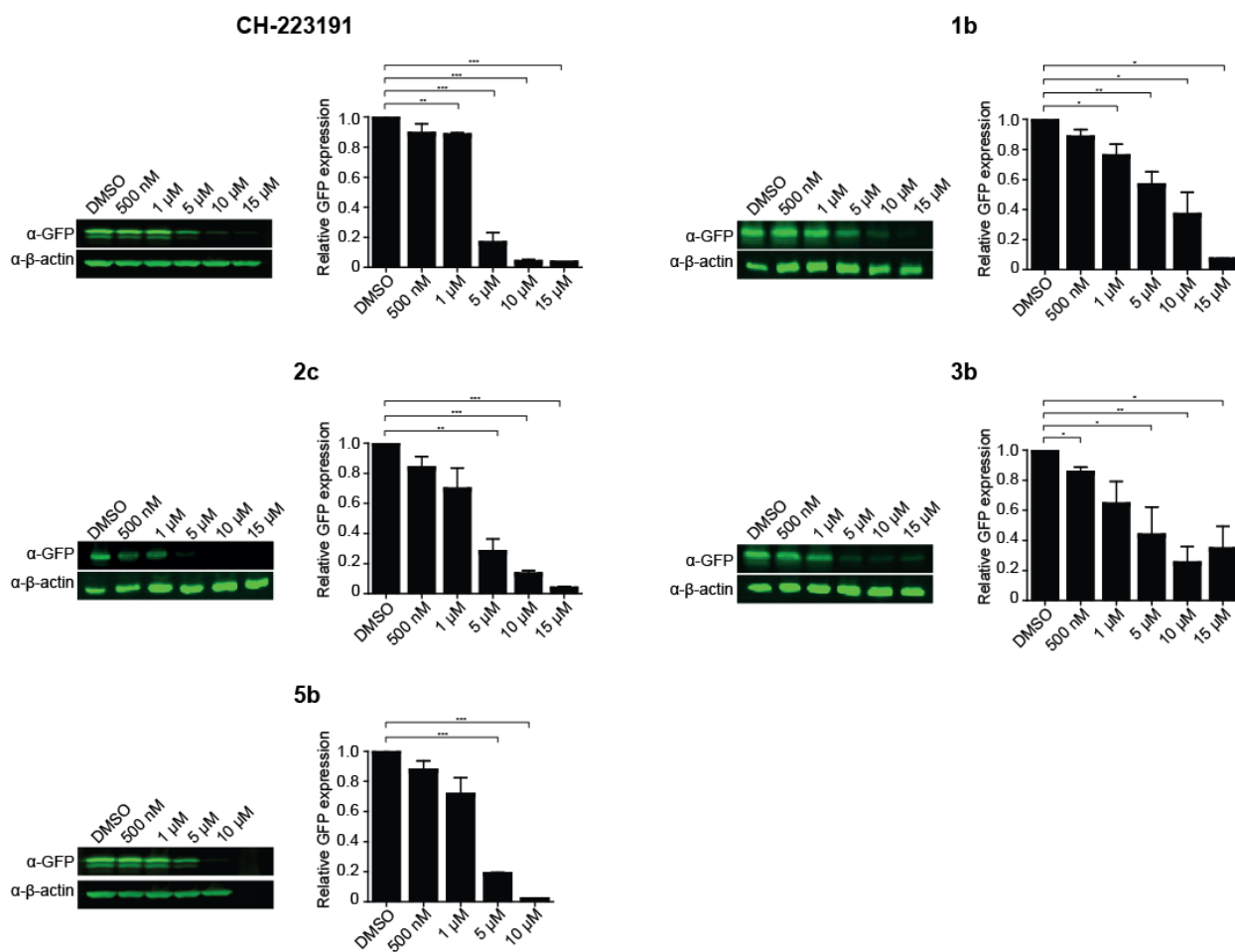
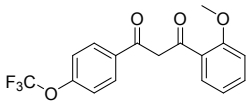
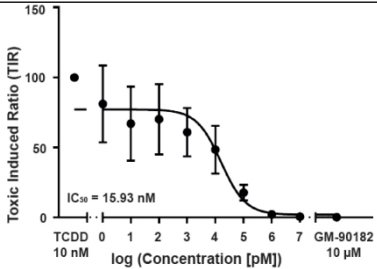
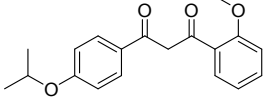
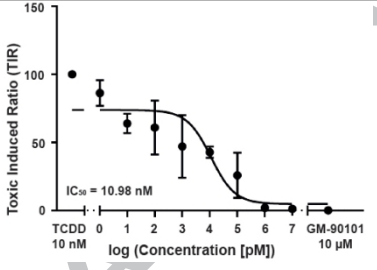
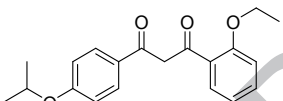
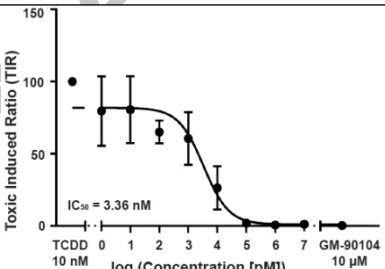
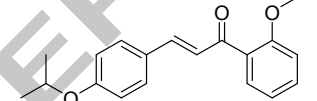
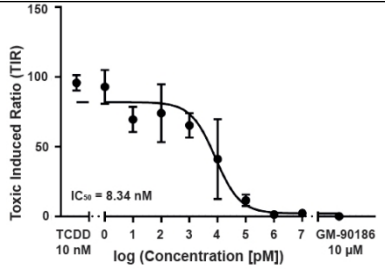
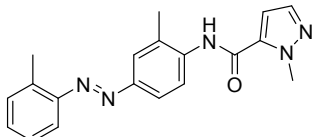
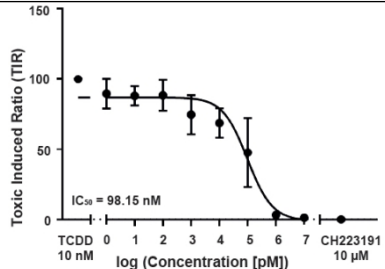


Fig. 5. Assessment of anti-AhR activity of compounds using GFP protein in *Tg(cyp1a:egfp)* zebrafish embryos. The embryos in Fig. 4 were subjected to Western blotting with anti-GFP antibody. Anti- β -actin antibody was used for a loading control. * $P < 0.05$; ** $P < 0.01$; *** $P < 0.001$ by the two-tailed Student's t -test.

Selected compounds were further evaluated in luciferase reporter gene AhR assay. The luciferase reporter assay indirectly measures AhR transcriptional activity by quantification of the luciferase expression in the mammalian cells induced by promoter of an AhR target gene. All investigational compounds showed better AhR antagonistic activity than the reference compound **CH223191**. Moreover, compounds **3b** and **5b** exhibited excellent in vitro activity with IC_{50} values of 3.36 nM and 8.3 nM, respectively (Table 4).

Table 4. IC₅₀ of AhR antagonists.

Compound	Structure		AhR antagonist activity (IC ₅₀)
1b			15.93 nM
2c			10.98 nM
3b			3.36 nM
5b			8.34 nM
CH223191			98.15 nM

Finally, we assessed the effect of the compounds on the expansion of HSCs. After 35 days of HSC culture with **individual compound**, CD34⁺ cells were counted. Compound **5b** exhibited more than 4 fold enhancements in cell number compared to media alone (Table 5). However, **1b**, **2c**, **3b** and CH223191 did not elicit significant change in cell number (data not shown).

Table 5. Haematopoietic stem cell expansion at 35 days after treatment with AhR antagonists.

Compound	Day 35 CD34 ⁺ number (x10 ⁶ cells)	
DMSO (0.01 %)	1.75	
5b	9.82	<p>Number of CD34⁺ (x 10⁶)</p> <p>DMSO GM-90186</p>

*** $P < 0.001$ by the two-tailed unpaired Student's t -test.

4. Conclusions

A new series of 1,3-diketone and α,β -unsaturated derivatives were identified and evaluated for their AhR antagonist activity using zebrafish and mammalian cells. Here, compounds **1b**, **2c**, **3b** and **5b** showed significant AhR antagonist activity in a transgenic zebrafish model. Among them, compound **3b** and **5b** were found to have excellent AhR antagonist activity with IC_{50} of 3.36 nM and 8.3 nM in luciferase reporter assay, respectively. In HSC proliferation assay, compound **5b** elicited marked HSC expansion.

5. Experimental section

5.1 Chemistry: general procedure

The reagents used in this study were purchased from commercial suppliers and used without further purification. Thin layer chromatography for analysis was performed using pre-coated silica gel glass plate (silica gel 60, F-254, 0.25 mm) of Merck. For the identification of the material separated on TLC, it was confirmed by UV lamp (254 nm and 365 nm). Merck silica gel grade 9385 (230-400 mesh) was used as a filler for the column for the purification of the reactants. For the determination of the structure of the synthesized compound, ¹H NMR spectra were run on JEOL JNMECS400 spectrometers at 400MHz. Chemical shift (δ) are expressed in ppm downfield from tetramethylsilane (TMS) as an internal standard, and CDCl₃, DMSO-d₆ were used as a solvent. The letters s, d, t, q and m are used to indicate singlet, doublet, triplet, quartet and multiplet. HRMS (EI) measurements were conducted at the Korea Basic Science Institute (KBSI).

5.2 Synthesis

5.2.1 Synthesis of methyl hydroxy benzoate (A).

Hydroxy benzoic acid and H₂SO₄ were in 50 ml MeOH. The resulting mixture was refluxed during 4 h, then cooled down to room temperature and concentrated in vacuo. The resulting residue was carefully quenched by NaHCO₃ saturated water solution and extracted with DCM. The combined organic layers were washed with brine, dried over Na₂SO₄ and the solvent were evaporated in vacuo.

5.2.2 Synthesis of methyl alkoxy benzoate (B).

To a solution of methyl hydroxy benzoate (1 eq) in dry THF were added alcohol (1 eq) and triphenylphosphine (PPh₃) (1.2eq). The reaction mixture was allowed to stir at 0 °C (ice bath) for 15 minutes. Diisopropyl azodicarboxylate (DIAD) (1.2 eq) was added dropwise into the cold solution and then stirred at room temperature for overnight under N₂. The mixture was diluted with water and extracted with ethyl acetate twice, and the combined organic phase was washed with brine solution, dried with Na₂SO₄, filtrated, and concentrated under reduced pressure. The residue was purified on a silica gel column.

5.2.3 Synthesis of alkoxy-acetophenone (C).

To a solution of hydroxyacetophenone (1eq) in dry THF were added alcohol (1 eq) and triphenylphosphine (PPh₃) (1.2 eq). The reaction mixture was allowed to stir at 0 °C (ice bath) for 15 minutes. Diisopropyl azodicarboxylate (DIAD) (1.2 eq) was added dropwise into the cold solution then stirred at room temperature for overnight under N₂. The mixture was diluted with water and extracted with ethyl acetate twice, and the combined organic phase was washed with brine solution, dried with Na₂SO₄, filtrated, and concentrated under reduced pressure. The residue was purified on a silica gel column.

5.2.4 Synthesis of 1,3-diketone derivatives.

To a suspension of sodium hydride (60% in mineral oil, 5 eq) in dry THF was added a solution of substituted methyl benzoate (2 eq) in dry THF. After mixture refluxed, substituted acetophenone (1 eq) in dry THF was added dropwise. The mixture was refluxed overnight, then quenched with 1N HCl. The mixture was extracted with ethyl acetate twice, and the combined organic phase was washed with brine solution, dried with anhydrous Na₂SO₄, filtrated, and concentrated under reduced pressure. The residue was purified on a silica gel column.

1-(2-Methoxyphenyl)-3-(4-(trifluoromethoxy)phenyl)propane-1,3-dione. (1b)

Using the procedure for 5.2.4 with methyl 2-methoxybenzoate and 4'-trifluoromethoxyacetophenone provided the title compound in 20.5% yield. ¹H-NMR (400 MHz, CDCl₃) δ 8.00 (dt, J = 9.3, 2.4 Hz, 2H), 7.95 (dd, J = 7.9, 1.8 Hz, 1H), 7.49 (ddd, J = 8.7, 6.9, 1.4 Hz, 1H), 7.34-7.28 (m, 2H), 7.12 (s, 1H), 7.11-7.05 (m, 1H), 7.02 (d, J = 8.2 Hz, 1H), 3.97 (s, 3H). ¹³C NMR (100 MHz, DMSO-d₆): δ 184.73 (C), 184.34 (C), 159.00 (C), 151.79 (C), 134.59 (CH), 134.42(C), 132.20 (C), 130.21 (C), 130.05(CH, CH), 123.93 (CH), 121.57(CH, CH), 121.16 (CH), 113.04(CH), 98.74(CH), 56.50 (CH₃). HRMS for C₁₇H₁₃F₃O₄ calcd, 338.0766; found, 338.0769 [M⁺].

1-(4-Isopropoxyphenyl)-3-(2-methoxyphenyl)propane-1,3-dione. (2c)

Using the procedure for 5.2.4 with methyl 4-methoxybenzoate and 2'-methoxyacetophenone provided the title compound in 66.1% yield. ¹H-NMR (400 MHz, CDCl₃) δ 7.97-7.90 (m, 3H), 7.49-7.42 (m, 1H), 7.11-7.04 (m, 2H), 7.00 (d, J = 8.5 Hz, 1H), 6.98-6.91 (m, 2H), 4.71-4.60 (m,

1H), 3.96 (s, 3H), 1.38 (d, J = 6.1 Hz, 6H). ¹³C NMR (100 MHz, DMSO-d₆): δ 186.61 (C), 182.18(C), 162.03 (C), 158.79 (C), 134.01 (CH), 131.07(CH), 130.01(CH), 129.98(CH), 127.55(C), 124.06(C), 121.10(CH), 115.99 (CH, CH), 112.93(CH), 97.71(CH), 70.24(CH₃), 56.46(CH₂), 22.18(CH₃, CH₃). HRMS for C₁₉H₂₀O₄ calcd, 312.1362; found, 312.1364 [M⁺].

1-(2-Ethoxyphenyl)-3-(4-isopropoxyphenyl)propane-1,3-dione. (3b)

Using the procedure for 5.2.4 with methyl 4-isopropoxybenzoate and 2'-ethoxyacetophenone provided the title compound in 10.0% yield. ¹H-NMR (400 MHz, CDCl₃) δ 8.01-7.97 (m, 1H), 7.93 (dt, J = 9.6, 2.4 Hz, 2H), 7.43 (ddd, J = 8.6, 6.9, 1.4 Hz, 1H), 7.26 (d, J = 1.2 Hz, 1H), 7.08-7.02 (m, 1H), 7.00-6.90 (m, 3H), 4.71-4.60 (m, 1H), 4.18 (q, J = 6.9 Hz, 2H), 1.55 (d, J = 6.1 Hz, 3H), 1.40-1.35 (m, 6H). ¹³C NMR (100 MHz, DMSO-d₆): δ 186.70 (C), 181.50(C), 162.03(C), 158.29(C), 134.08 (CH), 131.06(CH), 129.99 (CH, CH), 129.74 (C), 127.71(C), 123.63(CH), 121.00 (CH), 116.02 (CH), 113.62 (CH), 97.79 (CH), 70.24(CH₂), 64.59(CH₂), 22.19 (CH₃, CH₃), 15.19 (CH₃). HRMS for C₂₀H₂₂O₄ calcd, 326.1518; found, 326.1517 [M⁺].

5.2.5. Synthesis of chalcone derivatives.

To a substituted benzaldehyde in EtOH added NaOH at 0 °C (ice bath) then stir for 10 min. 2'-methoxyacetophenone was added slowly dropwise and the mixture was allowed to warm to room temperature overnight. The solvent was concentrated under reduced pressure. The residue was diluted with water and extracted with ethyl acetate twice, and the combined organic phase was washed with brine solution, dried with anhydrous Na₂SO₄, filtrated, and concentrated under reduced pressure. The residue was purified on a silica gel column.

(E)-3-(4-Isopropoxyphenyl)-1-(2-methoxyphenyl)prop-2-en-1-one. (5b)

Using the procedure for 5.2.5 with methyl 4-isopropoxybenzaldehyde and 2'-methoxyacetophenone provided the title compound in 90.0% yield. ¹H-NMR (400 MHz, DMSO-D₆) δ 7.66 (d, J = 8.9 Hz, 2H), 7.56-7.49 (m, 1H), 7.49-7.42 (m, 2H), 7.25 (d, J = 15.9 Hz, 1H), 7.18 (d, J = 8.5 Hz, 1H), 7.05 (t, J = 7.3 Hz, 1H), 6.96 (d, J = 8.9 Hz, 2H), 4.75-4.64 (m, 1H), 3.85 (s, 3H), 1.27 (d, J = 6.1 Hz, 6H). ¹³C NMR (100 MHz, DMSO-d₆): δ 192.67 (C), 160.09 (C), 158.07(C), 143.32 (CH), 133.23 (CH), 130.97 (CH, CH), 129.92 (C), 129.69(C), 127.28 (CH), 125.03(CH), 121.03 (CH), 116.32 (CH, CH), 112.79 (CH), 69.92(CH), 56.29 (CH₃), 22.24 (CH₃, CH₃). HRMS for C₁₉H₂₀O₃ calcd, 296.1412; found, 296.1414 [M⁺].

5.3. Zebrafish

Tg(cyp1a:egfp) zebrafish were maintained using standard procedures¹⁴ and staged in hours post-fertilization (hpf) as per standard criteria¹⁵.

5.3.1. A small molecule library screen using *Tg(cyp1a:egfp)* zebrafish

Tg(cyp1a:nls-egfp) embryos¹³ at 30 hpf were placed in 96 well-plates (three embryos per well; SPL Life Sciences) harboring E3 media (5 mM NaCl, 0.17 mM KCl, 0.33 mM CaCl₂·2H₂O and 0.4 mM MgCl₂·6H₂O, pH7.2) with 10 nM TCDD (catalog number: 48599; Sigma Aldrich) dissolved in DMSO. Each well contained three embryos and 200 µL of the media. Subsequently, 5 µM of 6,400 small molecules (Korea Chemical Bank) dissolved in DMSO were individually added to the well and incubated for 48 h. EGFP expression in the embryos were assessed under a fluorescent stereomicroscope (MZ16 FA, Leica). Efficacy of hit compounds and their derivatives dissolved in DMSO were tested in 2-ml glass vials (Suju Science) containing 10 embryos and 1-ml E3 media with 6 nM TCDD. CH-223191 (C8124, Sigma Aldrich) and StemRegenin1 (72342, STEMCELL Technologies), both of which are AhR antagonists, were used as a positive control.

5.4 Western blotting

Embryos were lysed with RIPA Lysis and Extraction Buffer (89900, Thermo Fisher Scientific), and the resulting lysates were separated by 10% sodium dodecyl sulfate polyacrylamide gel electrophoresis and then transferred to PVDF membranes (IPVH00010, Millipore). The membranes were incubated with anti-EGFP antibody (1:2,000; sc-9996, Santa Cruz Biotechnology) for 16 h at 4°C, washed with TBST (0.2 M Tris, 1.37 M NaCl and 0.1% Tween-20, pH 7.6) three times and probed with IRDye 800CW goat anti-mouse antibody (1:5,000; 925-32210, LI-COR Biosciences) for 1 h at room temperature. After washing with TBST, the membranes were imaged with an Infrared Imaging System (Odyssey CLx, LI-COR Biosciences).

5.5 DNA manipulation

To generate expression plasmids encoding zebrafish AhR, N- and C-terminal halves of AhR2 (GenBank Accession number NM_131264.1) were PCR-amplified from the cDNA with

specific primers (forward: 5'-AAG CTT ACC ATG TCG GCG GGT ATC GGT AC-3', reverse: 5'-CCT GCT TTA TAA ACA AGC CTA GCA TTG-3'; forward: 5'-GCT TGT TTA TAA AGC AGG AAG AC-3', reverse: 5'-ATC GAT GCG TAG TCA CAG CAG TTG CTT TG-3') and then simultaneously cloned into the HindIII/ ClaI sites of pCS4+-3xFLAG plasmid¹⁹. To construct expression plasmids encoding zebrafish AhR nuclear translocator (ARNT)-1c (NM_001045271.1), ARNT-1c was PCR-amplified from the cDNA with specific primers (forward: 5'-GCT AGC GGA TCC ACC ATG ACA TCA GCT AAT CCG-3'; reverse: 5'-GCT AGC CTC GAG TCA CTT GAC GTT GGT GTT GG-3') and cloned into the BamHI/XhoI sites of pCS4+ plasmid¹⁶. To generate zebrafish *cyp1a* reporter plasmids, two cis-regulatory regions (p-2608/-2100 and p-580/+71) within the *cyp1a* promoter¹⁷ were PCR-amplified from the genomic DNA with specific primers (forward: 5'-GCT AGC ACG CGT TAG AGC AGA ACT AGT GAA-3', reverse: 5'-GCT AGC CTC GAG TGT GAT GGT TTA GGC AAT-3'; forward: 5'-GCT AGC CTC GAG CTT TAA TCA GGG GTC GCT-3', reverse: 5'-ACT ATT AAG CTT CCG GAG CGA TCG AGT GGA-3') and then simultaneously cloned into the MluI/HindIII sites of pGL3-Basic vector (Promega).

5.6 Cell culture

COS-7 cells were cultured in RPMI1640 media (Welgene) supplemented with 10% fetal bovine serum (Welgene) and 1x Antibiotic-Antimycotic (Thermo Fisher Scientific) at 37°C and 5% CO₂ atmosphere.

5.7 Determination of the half maximal inhibitory concentration (IC₅₀) of compounds

IC₅₀ of compounds was determined as described previously¹⁸ with some modification. In brief, COS-7 cells were seeded onto 24-well plate at a density of 5 x 10⁴ cells/well. When reaching approximately 65% confluency, the cells were transfected with ARNT-1c expression plasmid (50 ng), AhR2 expression plasmid (5 ng), Cyp1a-firefly luciferase reporter plasmid (20 ng) and pRL-TK Renilla luciferase plasmid (Promega, 1 ng) using Lipofectamine 3000 (Thermo Fisher Scientific) according to the manufacturer's protocol. The pEGFP-C1 plasmid (Clontech) was used to assess the transfection efficiency. At 5 hr post transfection, compounds were added to the cells at various concentrations (1 pM, 10 pM, 100 pM, 1 nM, 10 nM, 100 nM, 1 μM and 10 μM). In parallel, TCDD (10 nM) or the compounds (10 μM) were added as a control. At 1 hr

post compound treatment, TCDD (10 nM) was added to all of the wells except the control wells. At 18 hr post TCDD treatment, the media was removed, and the cells were rinsed thoroughly with 500 μ l of Dulbecco's phosphate buffered saline (DPBS), treated with 100 μ l of 1x Passive Lysis Buffer (Promega) and rocked at room temperature for 15 min. The dual luciferase assay was carried out using a Dual-Luciferase Reporter Assay System (Promega) and an Orion L Microplate Luminometer (Titertek Berthold). The cell lysate (20 μ l) was mixed with the Luciferase Assay Reagent II (100 μ l), and the firefly luciferase activity was measured for 10 sec after a 3-sec delay. Subsequently, Stop & Glo Buffer plus Stop & Glo Buffer Substrate (100 μ l) was added and the Renilla luciferase activity was measured for 10 sec after a 3-sec delay. The ratio of firefly luciferase activity to Renilla luciferase activity was expressed as relative light unit (RLU) and RLU values were normalized and expressed as toxic induced ratio (TIR). IC₅₀ was determined using Prism (GraphPad Software).

5.8 Assessment of expansion of human CD34⁺ cells

Expansion of human CD34⁺ cells was assessed as described previously¹¹ with some modification. In brief, human CD34⁺ progenitor cells from cord blood (C-12921, PromoCell) were cultured in hematopoietic progenitor expansion medium DXF (C-28021, PromoCell) supplemented with 1x antibiotics (15240062, Gibco), Supplement Mix (C-39821, PromoCell) and Cytokine Mix E (C-39891, Promocell) containing recombinant human thrombopoietin, stem cell factor (SCF), Fms like tyrosine kinase 3 (flt-3) ligand and IL-3. The cells (5 x 10⁴ cells in 0.5 ml culture media) were seeded into 6-well plates (3471, Corning), and then immediately treated with compounds. Subsequently, the cells were transferred to 75-cm² flask (3814, Corning) and cultured at 37°C in 5% CO₂ for 5 weeks. The cell density was maintained between 5 x 10⁵ and 2 x 10⁶ cells/ml by adding fresh media. To count CD34⁺ cells, the cells were stained in staining media (PBS supplemented with 2% FBS and 2 mM EDTA) at 4°C for 1 h with anti-hCD34-APC (dilution ratio 1:50, 343608, BioLegend,) and anti-hCD45RA-FITC (1:50, 347723, BD Biosciences) or anti-hLin1-FITC (1:50, 348801, BioLegend) antibodies, washed with staining media and analyzed with flow cytometry (Accuri C6 instrument, BD Biosciences) at weeks 1 and 5. To perform a colony forming assay, cells were seeded into methylcellulose containing media (MethoCult SF H4436, 04436, StemCell Technologies) and cultured for 14 days. Colony forming units (CFUs) were scored under an inverted microscope (CKX41SF, Olympus). Colony

forming content of the expansion culture was calculated as follows: the average number of scored colonies from three dishes \times total mononuclear cell number/input cell number. Total mononuclear cells were determined by multiplying the number of cells per ml by the culture volume.

Acknowledgements

This work was supported by grants from the Ministry of Trade, Industry and Energy, Korea (2017-10063396), the Ministry of Science, ICT & Future Planning(MSIP)/National Research Foundation of Korea (NRF) (2016M3A9B6902868) and the Basic Science Research Program through the National Research Foundation of Korea (NRF) funded by the Ministry of Education (NRF-2013R1A1A2008587). The chemical library used in this study was kindly provided by Korea Chemical Bank (<http://www.chembank.org/>) of Korea Research Institute of Chemical Technology. Kun-Hee Kim thanks Health Fellowship Foundation for a graduate fellowship.

References

1. Bersten DC, Sullivan AE, Peet DJ, Whitelaw ML. bHLH-PAS proteins in cancer. *Nature Reviews Cancer*. 2013;13:827.
2. Okey AB. An Aryl Hydrocarbon Receptor Odyssey to the Shores of Toxicology: The Deichmann Lecture, International Congress of Toxicology-XI. *Toxicological Sciences*. 2007;98(1):5-38.
3. Nebert DW. Aryl hydrocarbon receptor (AHR): “pioneer member” of the basic-helix/loop/helix per-Arnt-sim (bHLH/PAS) family of “sensors” of foreign and endogenous signals. *Progress in Lipid Research*. 2017;67:38-57.
4. Fukunaga BN, Probst MR, Reisz-Porszasz S, Hankinson O. Identification of Functional Domains of the Aryl Hydrocarbon Receptor. *Journal of Biological Chemistry*.

- 1995;270(49):29270-29278.
5. Murray IA, Patterson AD, Perdew GH. Aryl hydrocarbon receptor ligands in cancer: friend and foe. *Nature Reviews Cancer*. 2014;14:801.
 6. Rothhammer V, Quintana FJ. The aryl hydrocarbon receptor: an environmental sensor integrating immune responses in health and disease. *Nature Reviews Immunology*. 2019;19(3):184-197.
 7. Mulero-Navarro S, Fernandez-Salguero PM. New Trends in Aryl Hydrocarbon Receptor Biology. *Frontiers in Cell and Developmental Biology*. 2016;4(45).
 8. Kerley-Hamilton JS, Trask HW, Ridley CJA, et al. Inherent and Benzo[a]pyrene-Induced Differential Aryl Hydrocarbon Receptor Signaling Greatly Affects Life Span, Atherosclerosis, Cardiac Gene Expression, and Body and Heart Growth in Mice. *Toxicological Sciences*. 2012;126(2):391-404.
 9. Pernomian L, da Silva CHTP. Current basis for discovery and development of aryl hydrocarbon receptor antagonists for experimental and therapeutic use in atherosclerosis. *European Journal of Pharmacology*. 2015;764:118-123.
 10. Casado FL, Singh KP, Gasiewicz TA. The aryl hydrocarbon receptor: Regulation of hematopoiesis and involvement in the progression of blood diseases. *Blood Cells, Molecules, and Diseases*. 2010;44(4):199-206.
 11. Boitano AE, Wang J, Romeo R, et al. Aryl Hydrocarbon Receptor Antagonists Promote the Expansion of Human Hematopoietic Stem Cells. *Science*. 2010;329(5997):1345.
 12. Kim S-H, Henry EC, Kim D-K, et al. Novel Compound 2-Methyl-2H-pyrazole-3-carboxylic Acid (2-methyl-4-o-tolylazo-phenyl)-amide (CH-223191) Prevents 2,3,7,8-TCDD-Induced Toxicity by Antagonizing the Aryl Hydrocarbon Receptor. *Molecular*

- Pharmacology*. 2006;69(6):1871.
13. Kim K-H, Park H-J, Kim JH, et al. Cyp1a reporter zebrafish reveals target tissues for dioxin. *Aquatic Toxicology*. 2013;134-135:57-65.
 14. Westerfield M. *The Zebrafish Book: A guide for the laboratory use of zebrafish (Danio rerio)*. Vol 5th ed. University of Oregon Press 2007.
 15. Kimmel CB, Ballard WW, Kimmel SR, Ullmann B, Schilling TF. Stages of embryonic development of the zebrafish. *Developmental Dynamics*. 1995;203(3):253-310.
 16. Jin Y-H, Jeon E-J, Li Q-L, et al. Transforming Growth Factor- β Stimulates p300-dependent RUNX3 Acetylation, Which Inhibits Ubiquitination-mediated Degradation. *Journal of Biological Chemistry*. 2004;279(28):29409-29417.
 17. ZeRuth G, Pollenz RS. Functional analysis of cis-regulatory regions within the dioxin-inducible CYP1A promoter/enhancer region from zebrafish (*Danio rerio*). *Chemico-Biological Interactions*. 2007;170(2):100-113.
 18. Bak S-M, Iida M, Hirano M, Iwata H, Kim E-Y. Potencies of Red Seabream AHR1- and AHR2-Mediated Transactivation by Dioxins: Implication of Both AHRs in Dioxin Toxicity. *Environmental Science & Technology*. 2013;47(6):2877-2885.